Pergamon

Acta mater. 49 (2001) 1261–1269

Acta MATERIALIA

www.elsevier.com/locate/actamat

IN SITU OBSERVATION OF HOT TEARING FORMATION IN SUCCINONITRILE-ACETONE

I. FARUP[1, 2], J. -M. DREZET[1] and M. RAPPAZ[1]†

[1]Laboratoire de Métallurgie Physique, Ecole Polytechnique Fédérale de Lausanne, MX-G CH-1015, Lausanne, Switzerland and [2]SINTEF Materials Technology, P.O. Box 124, Blindern N-0314, Oslo, Norway

(Received 12 September 2000; received in revised form 12 December 2000; accepted 17 December 2000)

Abstract—Hot tears have been induced during the solidification of a succinonitrile-acetone alloy by pulling the columnar dendrites in the transverse direction with a pulling stick. The opening of the mushy zone (hot tears) always occurred at grain boundaries. At low volume fraction of solid, the opening can be compensated by leaner-solute interdendritic liquid (i.e., "healed" hot tears). At higher volume fraction of solid, hot tears directly nucleate in the interdendritic liquid or develop from pre-existing micropores induced by solidification shrinkage. Their surface (edge) is made of secondary dendrite arms, which have not yet bridged, but a few spikes have also been observed. These later spikes formed either by the necking of solid bridges established across the grain boundaries prior to pulling, or by the sudden break-up of the liquid film during pulling. Similar spikes have been found by SEM on the hot tear surface of an aluminium–copper alloy. © *2001 Published by Elsevier Science Ltd on behalf of Acta Materialia Inc.*

Keywords: Casting; Defects; Organic alloys; Aluminium

1. INTRODUCTION

Hot tearing or hot cracking is a problem commonly encountered during the casting of large freezing range alloys. Over the last several decades, much effort has been put into the understanding of the underlying mechanisms and several theories have been proposed. Pellini [1] stated that hot tearing will occur if the material is subjected to an excessive accumulated strain within the so-called vulnerable part of the solidification interval. Guven and Hunt [2] and Campbell [3] also emphasised the role of tensile stresses in the formation of hot tears. Nevertheless, most hot tearing criteria neglect the importance of thermomechanical aspects and simply consider the solidification interval of the alloy [3]: the larger the freezing range, the more susceptible the alloy will be to hot tearing. Clyne and Davies [4] defined a more refined criterion in which the time interval spent by the mushy zone in the vulnerable region appears. This region corresponds to the existence of a thin continuous film of interdendritic liquid in between the dendrite arms and thus also to a low permeability (volume fractions of solid in the range of 0.9–0.99). When thermal strains are induced in this region by the coherent solid underneath, this film is not able to sustain the stresses and an opening will form if liquid cannot be fed to these regions. Feurer [5] focused instead on the liquid present in between the grains and argued that a hot tear will nucleate as a pore if the liquid is no longer able to fill the intergranular openings. Unfortunately, he only considered the contribution of solidification shrinkage. Rappaz *et al.* [6] recently extended this approach in order to also take into account the feeding associated with tensile deformation of the solidified material in the direction transverse to the dendritic growth. Farup and Mo [7] formulated a two-phase model of a deforming, solidifying mushy zone where both interdendritic liquid flow and thermally induced deformation of the solid phase were also taken into account. The reader is referred to Sigworth [8] for a more detailed review of hot-tearing theories.

Scanning Electron Microscopy (SEM) investigations have been made of hot tear surfaces in metallic alloys—see, e.g., References [3, 4]—and much of our knowledge in this field is based upon such studies. They all revealed the bumpy nature of hot tear surfaces, made of secondary dendrite arm tips, and clearly showed that hot tears form as interdendritic openings near the end of solidification in the mushy zone. In some cases, phases having grown on the tear surface after the interdendritic opening can

† To whom all correspondence should be addressed. Tel.: +41-21-693-2844; Fax: +41-21-693-5890.
E-mail address: michel.rappaz@epfl.ch (M. Rappaz)

1359-6454/01/$20.00 © 2001 Published by Elsevier Science Ltd on behalf of Acta Materialia Inc.
PII: S1359-6454(01)00013-1

be observed. Analysing these phases in the case of a commercial aluminium alloy, Nedreberg [9] confirmed that hot tears indeed form during the last stage of solidification. Spikes of a size of about 10 μm have been observed on the tear surfaces by Clyne and Davies [4], Spittle and Cushway [10], and recently by Drezet *et al*. [11]. These spikes are generally taken as evidences of solid bridges between the primary grains, which have been elongated during hot tearing.

Although *ex situ* investigations on cracked surfaces abound, *in situ* observations of hot-tear formation are rare because of the technical problems involved with metallic alloys. Recently, Herfurth and Engler [12] developed a technique where an aluminium–copper alloy could be pulled apart during solidification between two silica-aerogel plates while directly observing. Unfortunately, their technique at the present stage only allows for the macroscopic study of crack formation at high temperature.

In the present study, an organic model alloy of succinonitrile (SCN) and acetone is used to visualise in situ hot tear formation during solidification. In Section 2, the experimental technique is described, while Section 3 presents some of the results obtained, usually in the form of a sequence of recorded video images. For the sake of comparison with spikes formed in a metallic alloy, a hot-tear surface in aluminium–copper is also examined with SEM.

2. EXPERIMENTAL TECHNIQUES

Due to its attractive properties such as transparency, low entropy of fusion, BCC lattice, and convenient melting temperature (see Table 1), the SCN-acetone system has been used extensively in the past for the study of solidification [13]. Just like aluminium alloys [14], it is known to exhibit steady-state power-law creep at temperatures close to and below the solidus for the low strain rates encountered during common casting processes [15]. It has also been used for the study of fragmentation of the mushy zone [16]. This alloy, which has a solidification shrinkage similar to that of aluminium, is used in the present study to induce hot tearing.

The basic idea of the experiment is to set up a stationary mushy zone with only one layer of growing dendrites in order to directly observe crack opening and liquid feeding. The design of the experiment (see Fig. 1), is very similar to that described in Reference [13]. Two glass plates (76×26 mm^2) are held apart by a rectangular 100-μm thick TEFLON frame spacer. For recording the temperature profile during the experiment and for determining the composition of the organic alloy, a type-K thermocouple with a wire diameter of 50 μm is inserted in the cell together with a pulling stick. This puller is used to deform the mushy zone perpendicularly to the growth direction. It is made of 100-μm thick MYLAR sheet. This material was selected for its strength sufficient to provide the pulling force, its thermal conductivity similar to that of SCN [19], and its adhesion to the solid SCN. After gluing the glass plates and spacer, the cell was filled by capillarity with the molten alloy.

During the directional solidification experiment, the cell is placed upon two water-cooled copper plates. Underneath the middle part of the cell, a resistance heating wire can melt locally the alloy during the experiment. A motor and gear system ensures that the cell is moving at a constant speed in the thermal gradient supplied by this heating/cooling system. The experiments are performed in air and the solidification of the dendrites as well as the formation of hot tears can be observed through a microscope. The photographs shown in this paper are still pictures obtained from the videotapes recorded during the experiments by a video camera attached to the microscope.

After a rest period of about 30 min to establish a thermal equilibrium between the heated wire and the cooled plates, the cell is moved at constant velocity. When the solidification front approaches the MYLAR puller, the puller is repositioned so that it is close to—but not across—a grain boundary (typical distance:

Table 1. Relevant material parameters for the SCN-acetone system

Reference melting point	T_{mp}	58.08°C	[17]
Entropy of fusion	Δs_f	1.4 10^5 J K^{-1} m^{-3}	[18]
Slope of liquidus	m	−2.8 K wt%$^{-1}$	[13]
Partition coefficient	k	0.1	[13]
Solidification shrinkage	β_s	0.047	[18]

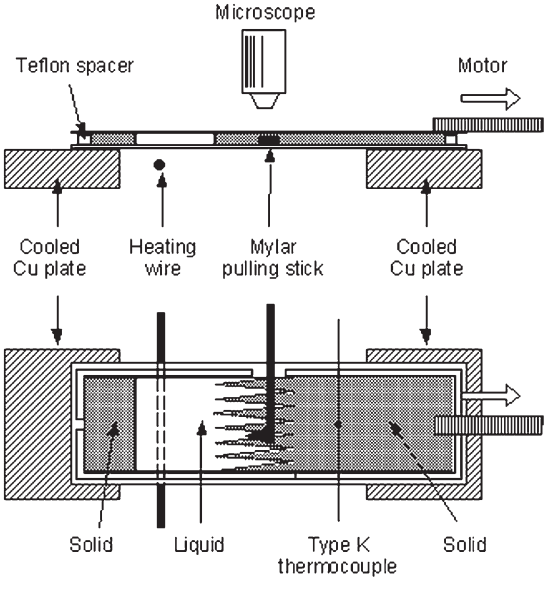

Fig. 1. Schematic drawing of the experimental set-up in side view (top) and from above (bottom).

0.1–1 mm). Pulling is performed manually when the puller is completely surrounded by solid material and the primary dendrites around the puller are more or less fully coalesced within a grain. Therefore, liquid only remains as a continuous film at the grain boundaries and as isolated drops in between the coalesced dendrite arms. When pulling is too early, liquid is able to fill the opening, whereas when it is too late, it becomes impossible to successfully open the network at a grain boundary, and the deformation is localised around the puller. Usually, only 2–4 experiments are performed with a given cell.

The concentration of the alloy, as determined from the measured liquidus temperature and the phase diagram (Table 1), varied between 0.5 and 5 wt.% acetone. The solidification rate was in the range 5–70 μm/s. The thermal gradient, determined by the temperature difference between the maximum value measured at the heating wire position and that imposed at the copper plate, was of the order of 17–31 K/cm.

3. RESULTS AND DISCUSSION

3.1. Preliminary experiments

During preliminary experiments, pulling was applied at various stages of solidification (i.e., at various volume fractions of solid). It was observed that deformation was always localised at grain boundaries unless pulling was applied at a very early stage of solidification. Furthermore, the separation of primary dendrite trunks belonging to a single grain was almost impossible to achieve. This is closely related to the fact that secondary dendrites arms belonging to a single grain (i.e., having the same crystallographic orientation) coalesce at a much earlier stage of solidification than those located on both sides of a grain boundary (i.e., having different crystallographic orientation).

A typical scenario when pulling is performed at a fairly early stage of solidification is shown in Fig. 2 for three different instants, Fig. 2(d) showing a schematic representation of the final situation [Fig. 2(c)].† The tip of the pulling stick (A) is seen on the right hand side of the figure, and the pulling direction is upwards. The solidification front is moving towards the left and is positioned at some distance to the left of the picture. Since the materials observed under the microscope (solid/liquid SCN, glass plate, bubble) are transparent, the *interfaces* between two phases and perpendicular to the glass plate are actually seen (e.g., solid–liquid interface, interface between a bubble and either the liquid or the solid SCN), as a result of a change in the refraction index.

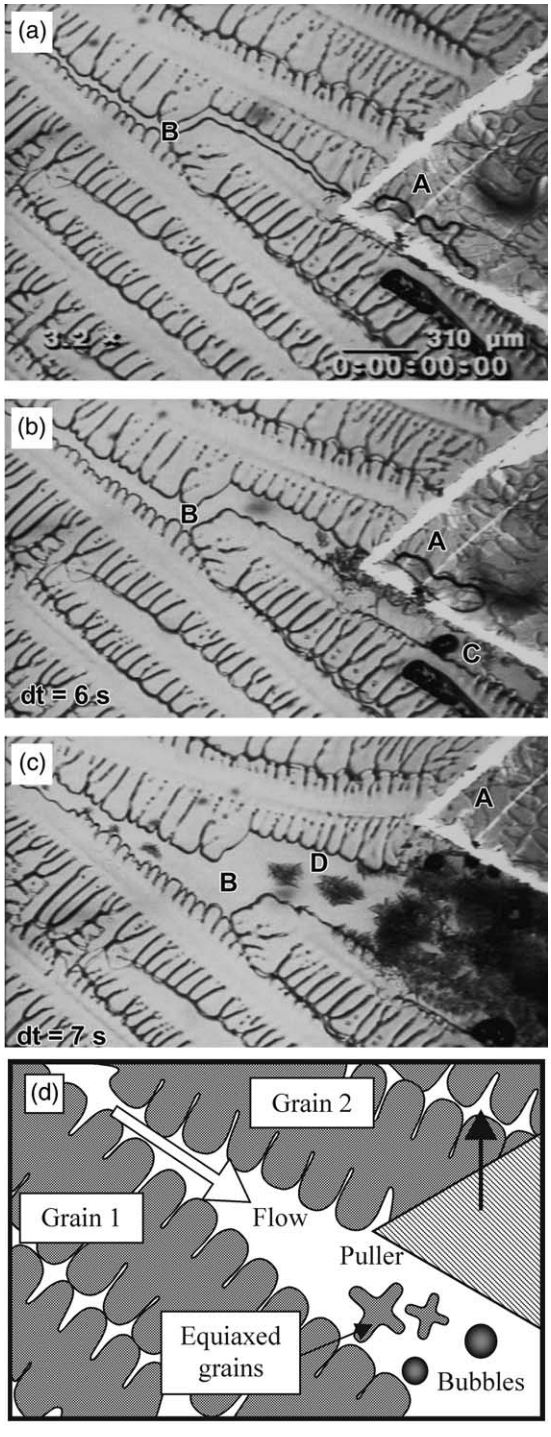

Fig. 2. Sequence showing an intergranular opening which is filled with undercooled liquid: (a) Initial configuration of grain boundary; (b) after pulling about 100 μm in the upper direction within 6 s; (c) after pulling an additional 100 μm in only 1 s. The scale is shown in (a), whereas the elapsed time, d*t*, since the beginning of the pull is indicated in each figure. Nucleation of pores (C) and of equiaxed grains (D) can be observed; (d) Schematic representation of the situation seen in (c) with the liquid in white, the two columnar grains and the tiny equiaxed grains in grey and the spherical bubbles in shaded grey. The black arrow indicates pulling direction.

† In this preliminary experiment, a more transparent puller of polyethylene was used instead of MYLAR. Since the thickness of this puller did not exactly match the spacing left between the two glass plates, dendrites have grown both above and below the puller.

From the orientation of the primary dendrite trunks, it is apparent that two grains are present in this experiment. The grain boundary, labelled (B) in Fig. 2, is characterised by a fairly large amount of interdendritic liquid, whereas the dendritic network within any of the two grains is already fairly compact. Please note however that the dendrite arms have not yet coalesced at this stage, even within the grains. Figure 2(b) shows the situation after pulling slowly approximately 100 μm in the upper direction during 6 s. The grains are slightly more separated, but liquid from the solidification front was able to feed the gap almost entirely. However, due to the pressure drop associated with the suction of the liquid, a pore has formed near the puller (C). The pore can be clearly distinguished on the picture by the much darker interface present between the liquid and the gas phase. Figure 2(c) shows the situation one second later, after pulling about 100 μm more with much higher velocity. Several pores have formed due to the increased depression associated with the increased pulling speed, in agreement with the analysis of Rappaz *et al*. [6]. Equiaxed grains (D) have also spontaneously nucleated in this intergranular liquid when solute-lean melt coming from regions closer to the dendrite tip front was suddenly sucked in this cooler region.† Such filled gaps between grains, commonly referred to as "healed" or "filled" hot tears, can be observed in as-cast products of metallic alloys [3].

When pulling is performed at even higher solid fractions than in the previous example, the feeding difficulty becomes so strong that a hot tear will form. Examples of this are shown in Figs 3–6 and are discussed in greater details below. It should be pointed out before that in six of the cells, in which the amount of acetone was below 1.5 wt.%, hot tears were formed, whereas in the six other cells having higher solute concentrations, no tears could be initiated under similar pulling conditions. From this, a rough estimate of an upper limit of the liquid fraction for hot-tear formation could be found assuming Scheil solidification (no diffusion of acetone in solid SCN). It is found that the remaining fraction of liquid when the tears form at the cold side of the mushy zone (30°C) could be as high as 0.12 for a concentration of 1.5 wt.% of acetone. However, this result should be taken with some care since the experimental conditions were not controlled so accurately (e.g., pulling speed, levels of acetone and humidity in the cell, etc.).

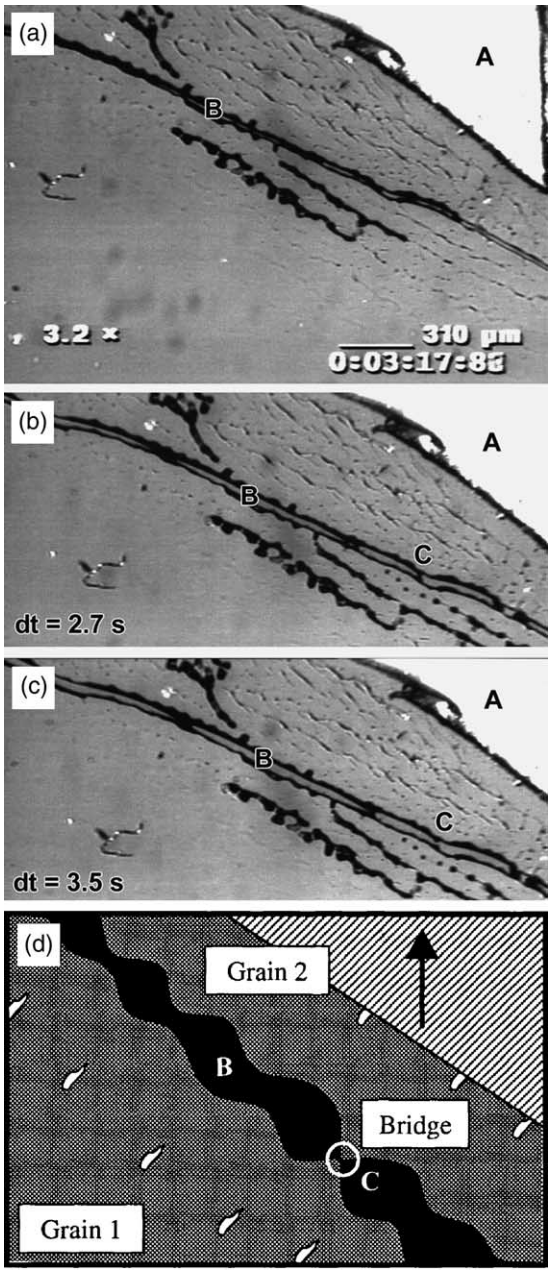

Fig. 3. Sequence showing direct nucleation of a hot tear as an elongated pore at a grain boundary (B). Spikes (C) are formed on the tear surfaces from solidified bridges. The elapsed time, d*t*, since the situation shown in (a) is indicated in each figure; (d) schematic representation of the necking of two dendrite arms which have bridged before pulling (empty hot tear is in black).

3.2. Nucleation of hot tears

Several nucleation mechanisms of hot tears were observed in the experiments. The most common one is illustrated in Fig. 3, showing the lower part of the puller (A) and a grain boundary (B). As compared with Fig. 2, Fig. 3 has been taken deeper in the mushy zone and where the secondary arms of dendrites belonging to a given grain are now well coalesced. Interdendritic boundaries containing still some liquid appear as wavy darker lines within the grains. In Fig. 3(a), the tear has just nucleated directly as a long pore on the grain boundary (B). The black lines/spots above and below the grain boundary are small pores

† It could be argued that solute-lean liquid is also coming from warmer zones, thus preventing nucleation of equiaxed grains. However, even in SCN, thermal equilibrium is reached much faster than the equilibrium of solute species (high Lewis number).

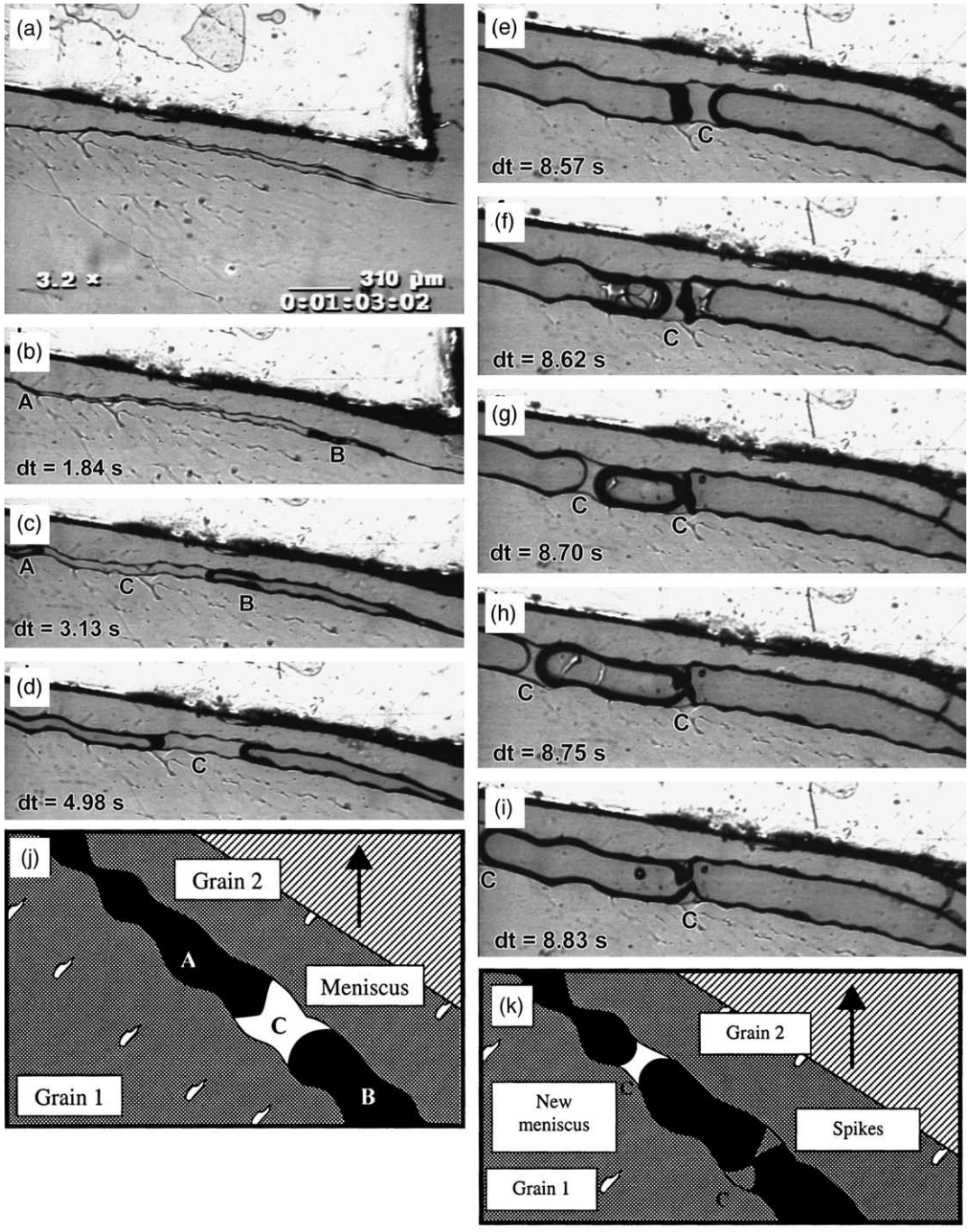

Fig. 4. Sequence showing nucleation of a hot tear as two pores in an initially healed hot tear. Spikes are formed where the two pores meet by sudden breaking of the remaining liquid film (see text). The elapsed time, d*t*, since the situation shown in (a) is indicated in each photograph; (j) and (k) schematic representations of the stretching of a liquid meniscus (in white) between two grains (in grey, empty hot tear is in black) corresponding to photographs (e) and (g), respectively.

which form between the glass plates and the solidified SCN-alloy—sometimes as a result of solidification shrinkage, but mainly due to the pressure drop associated with pulling. The following evolution of the tearing shown in Fig. 3(b) and (c) will be discussed in Section 3.3 and is summarised in Fig. 3(d).

Another common nucleation mechanism of hot tears is shown in Fig. 4(a–d). In this case, the puller is positioned just above a grain boundary, and Fig. 4(a) shows the situation just after starting to pull. The pulling was so slow that liquid was just able to flow from the solidification front to fill the gap, leaving a healed hot tear in Fig. 4(a). Slightly later [Fig. 4(b)], feeding of the opening becomes so difficult that two

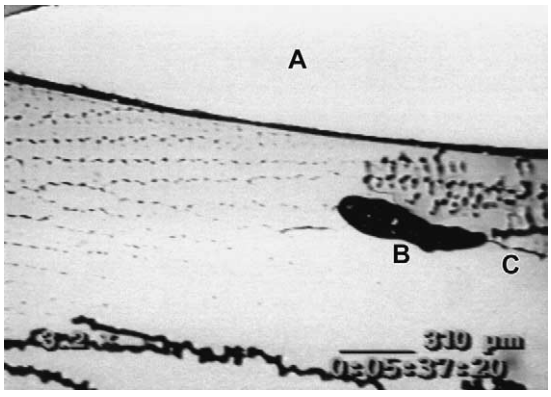

Fig. 5. Nucleation of a hot tear on a pore caused by solidification shrinkage and located at a grain boundary.

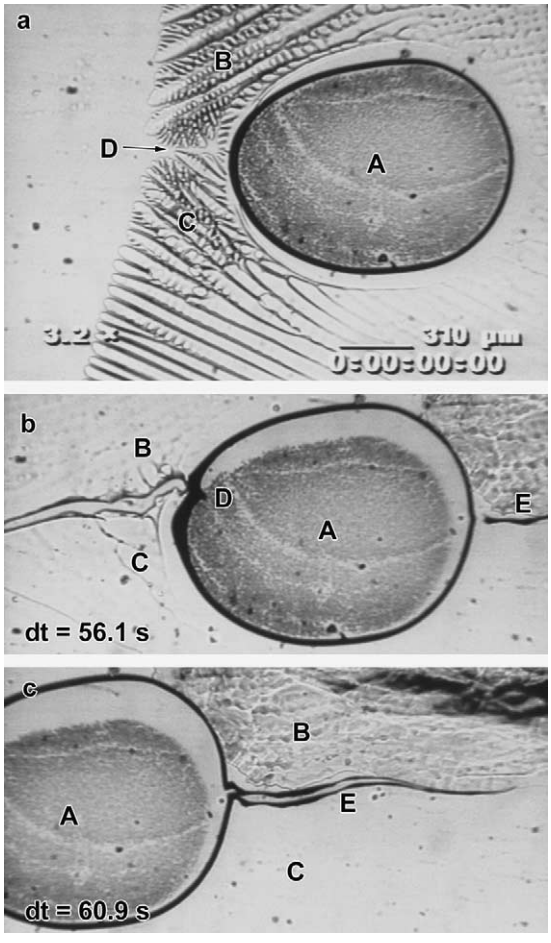

Fig. 6. Sequence showing: (a) The dendritic growth of two grains (B) and (C) around a pre-existing bubble (A). At the grain boundary (D) a zone of strong segregation has passed the bubble. Upon pulling (b) a healed hot tear forms on the left side of the bubble and extends up to the dendrite tips. On the right of the bubble, a hot tear (E) has nucleated at the grain boundary, but connects only later to the bubble (c). The elapsed time, d*t*, since (a) is shown in each figure.

pores have nucleated on both ends of the healed hot tear (locations labelled (A) and (B)), i.e., precisely in the regions where the required nucleation undercooling for pore formation is minimum. These pores grow inwards in the remaining liquid as the two grains are pulled apart [Fig. 4(c) and (d)] and at the end constitute the hot tear. The remaining pictures in this sequence will be explained in Section 3.3.

Figure 5 shows a special type of hot tear nucleation which was observed in only one case.† The puller (A) is positioned just above a grain boundary, on which a pore (B) caused by solidification shrinkage is already present before pulling. Upon pulling, a tear (C) is initiated directly from this pore and grows along the grain boundary and eventually develops as a hot tear. In this case, the pore thus acts as a nucleation point for the hot tear.

A situation often encountered in the experiments is shown in Fig. 6. A macroscopic bubble (A) with a diameter of about 1 mm is existing in the melt prior to the experiment. Such bubbles can be caused by poor filling of the cell or by earlier experiments with pulling. In the case shown in Fig. 6, the bubble is positioned at a grain boundary (D) between the two grains (B) and (C). The bottom of the puller is just above the picture (not seen). In Fig. 6(a), it can be observed that the solid SCN dendrites wet very well the bubble on both sides, i.e., the interfacial energy between the bubble and the solid is lower than that between the liquid and the bubble. This sharpens the dendrite tip and makes it grow along the bubble boundary instead of keeping a defined crystallographic direction (usually <100> in FCC and BCC materials) [see Fig. 6(a)]. Since rejection of solute is made easier when the tip is sharper, the two dendrites growing along the bubble have a slightly smaller undercooling and lie slightly ahead of dendrites growing within the grains. The impingement of the two dendrites growing on each side of the bubble and the restoration to a normal steady-state regime [region D in Fig. 6(a)] creates a segregated region at the grain boundary. Similar growth phenomena close to wetting surfaces have been discussed in detail by Fabietti *et al.* [20] and have been simulated recently with the phase-field method by Sémoroz *et al.* [21]. Figure 6(b) shows the situation much later when the material around the bubble is more or less coalesced and the puller has been moved a distance of approximately 130 μm. Several interesting observations can be made in this picture. First, the bubble has expanded significantly due to the pulling, as can be seen from the deposit on the glass plate indicating the original size and shape of the pore. Secondly, a healed hot tear extending up to the dendrite tips has formed on the strongly segregated grain boundary on the left-hand side of the bubble. On the right hand side towards the

† The authors apologize for the poor contrast of this picture caused by inappropriate settings on the video camera.

colder region and dendrite roots, a real hot tear has nucleated (E). It should be noted that the tear does not nucleate directly on the bubble as it did on the pore (Fig. 5), but rather as a separate hot tear on the grain boundary to the right of the bubble as in Fig. 3. It connects to the bubble about 3 s later [Fig. 6(c)].

Pre-existing bubbles and shrinkage porosity behave quite differently with respect to the nucleation of hot tears, mainly through the different coalescence behaviour of dendrite arms in these regions. In the case of a bubble (Fig. 6), coalescence of dendrite arms behind the bubble is clearly favoured by the existence of a triple junction (solid–liquid–bubble) early in the solidification process when there is enough liquid. As demonstrated by the preferred growth of dendrites along the sides of the bubble, the solid wets better the bubble as compared with the liquid and surface energy is minimised by having only solid in contact with air. On the opposite, the formation of shrinkage porosity at a late stage of solidification does not influence the coalescence behaviour of the dendrite arms.

3.3. Forming of spikes on the hot tear surface

Spikes similar to those observed by SEM at the surface of hot tears in metallic alloys could also form in the SCN alloys investigated here. However, two different formation mechanisms have been identified: (i) necking of bridged dendrite arms, a mechanism already invoked for metallic systems [4, 10, 11], and (ii) rupture of a liquid meniscus. These two mechanisms are explained below.

In Fig. 3(a), the tear is initially made out of one long pore extending throughout the entire intergranular opening. The black regions observed between the grains in Fig. 3(b) are regions where the solid is connected, suggesting intergranular coalescence or bridging [see also the schematic diagram of Fig. 3(d)]. They are black due to the fact that they do not fill entirely the space between the two glass plates, i.e., a small horizontal air gap exists between the solid and the glass plate. Upon further pulling [Fig. 3(c)], the bridge (C) of Fig. 3(b) is deformed and finally breaks up in two spikes facing each other.

During the sequence of Fig. 4, two pores nucleated at both extremities of a healed hot tear, as discussed in the previous section. As the two grains are pulled further apart [Fig. 4(c) and (d)], the two pores grow while the interdendritic liquid in between nearly remains constant in volume but is stretched in the pulling direction (zone C). As can be seen in Fig. 4(e) from the shape of the meniscus, solidification has already started on the left side of the liquid bridge [non-spherical shape of pore A extremity in Fig. 4(e)], while it is still fully liquid on the right (spherical shape of pore B extremity). This situation is also illustrated schematically in Fig. 4(j) (partially solidified liquid meniscus in white, pores in black and the two grains are grey). At this stage, the imposed separation between the two grains does not allow the fixed volume of liquid to maintain equilibrium conditions at the triple junction with the pore and the solid. Upon further pulling [Fig. 4(f)–(i)], the liquid part of the meniscus breaks away within a few hundredths of a second almost as a shock wave [Fig. 4(f)]. The part of the meniscus that was already solid at that time remains at the same location [previously labelled C in Fig. 4(f)]: it leaves two spikes on the two opposite surfaces of the hot tear [Fig. 4(g)]. Due to the loss of surface tension equilibrium during breakage, the liquid on the right part of the former meniscus has moved to the left and has rebuilt as a new meniscus (also labelled C). In between the spikes and the new meniscus, a bubble is also present, as shown schematically in Fig. 4(k). Please note that this new liquid meniscus continues to move to the left with the initial momentum gained during breakage [Fig. 4(g)–(i)]. It will settle in a narrower region of the hot tear (not shown in these pictures), where mechanical equilibrium can again be established between the capillary forces. Although the sequence of events shown in this figure is certainly influenced by the presence of the two glass plates, a similar mechanism could probably happen in real hot tears observed in metallic systems.

In order to better understand which of the two mechanisms mentioned above contribute to spike formation in metallic alloys, the spikes recently found by Drezet *et al*. [11] were further examined. These spikes were formed on a hot-tear surface obtained in an aluminium–copper 3 wt.% alloy solidified on a cooled central cylinder (ring mould test, Ref. [11]). The hot tear was then examined using stereo microscopy and SEM, after washing the specimen in an ultrasonic bath of acetone in order to remove dirt. In one small region, the spikes shown in Fig. 7 were found. These spikes exhibit a characteristic draped-looking shape, which is especially pronounced near the root (see enlargement of spike (A) at the bottom of the figure). This might be what remains of an oxide layer on the liquid–gas interface. No traces of plastic deformation can be observed on these spikes, indicating that they are formed by the second of the mechanisms described above, i.e., by partial solidification of a liquid bridge connecting two grains.

The liquid-bridge mechanism, as the other mechanism involving elongation of a solid bridge, requires to have spikes facing each other on each side of the hot tear surface. This is verified in Fig. 8, for which the two hot tear surfaces have been enlarged and mounted facing each other. The points labelled A and B allow to identify the parts of the hot tear surfaces. As can be seen, spikes labelled C, D, E are clearly facing each other.

Another spike type found in the same hot tear is shown in Fig. 9†: an intergranular solid bridge has

† Please note that another spike, facing the one shown in Fig. 9, was found on the other surface of the hot tear.

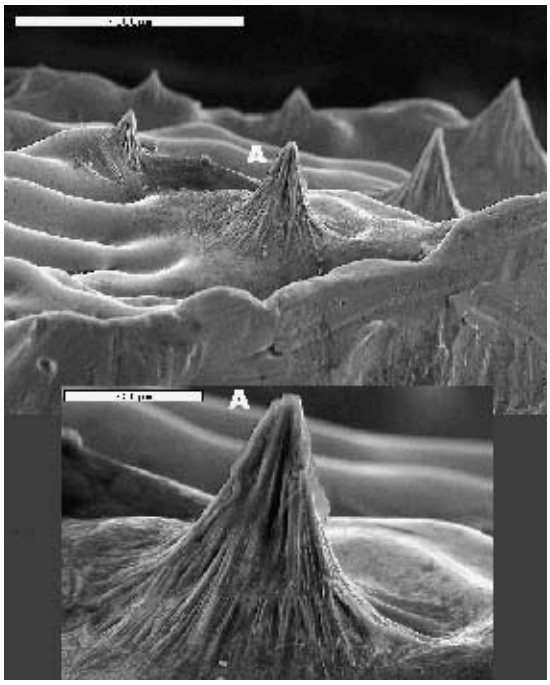

Fig. 7. SEM picture with close-up of draped-looking shape spikes on a hot tear surface in an Al-3 wt.% Cu alloy.

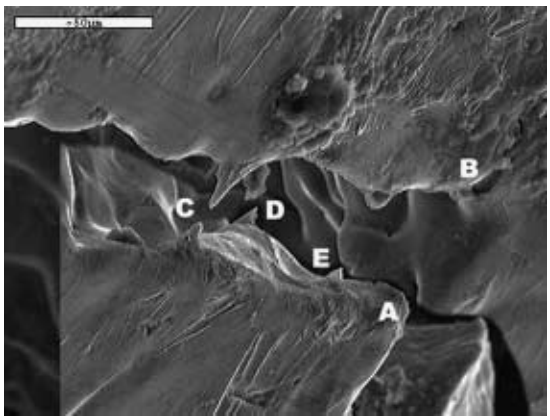

Fig. 8. Mounting SEM pictures of the two surfaces of a hot tear in an Al-3 wt.% Cu alloy showing the corresponding positions of the spikes (C, D, E).

been clearly deformed during the opening of the hot tear. This is obvious from the strongly deformed surface of the spike (see enlargement of region (A) at the bottom of Fig. 9). However, the very bottom of this spike (enlargement of region (B)) has the same draped-like appearance observed in the previous figures. Thus, it is most likely that this spike was formed initially by the same mechanism shown in Fig. 4, i.e., the initial formation of a liquid meniscus across the grain boundary. However, this meniscus has solidified in such a way that the two solid parts coming from each side have coalesced before break-up of the meniscus. This solid bridge was subsequently deformed during further pulling.

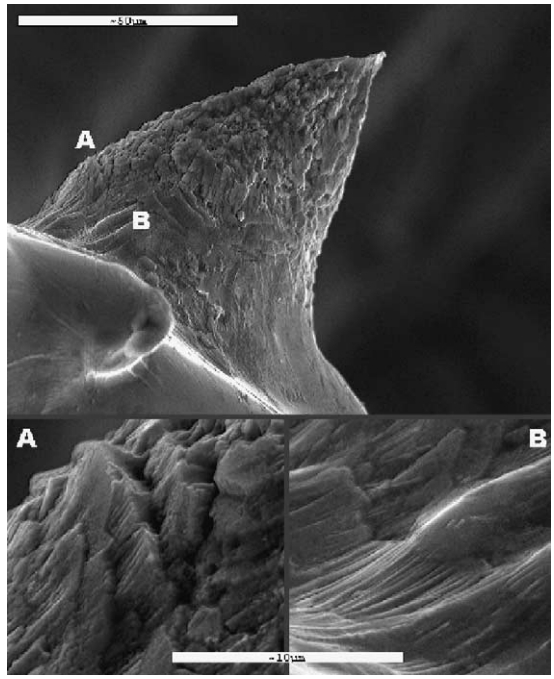

Fig. 9. SEM image with close-ups of a torn-apart solidified bridge on a hot tear surface in an Al-3 wt.% Cu alloy showing a deformed surface structure on the main part of the spike (region A), and an undeformed draped-looking shape near the root (region B).

4. CONCLUSIONS

In summary, these in situ observations in organic alloys have allowed to identify some of the mechanisms responsible for hot tearing nucleation and spike formation. At least, three different mechanisms for tear nucleation have been identified: (1) directly as elongated pores or tears, (2) on pores caused by solidification shrinkage, or (3) as round pores nucleated in the liquid constituting a healed hot tear. On the other hand, it seems that the major mechanism of spike formation in metallic alloys is the formation of a liquid meniscus joining the two grains which are pulled apart. This mechanism has been observed in situ in organic alloys and can be understood fairly easily by considering the difficulty of coalescence that two grains of different crystallographic orientations can have. The continuous film of liquid located at a grain boundary can thus remain up to a very late stage of solidification. Upon pulling, this continuous film becomes a liquid meniscus within which solidification proceeds up to the disruption of the film by surface tension forces. In some cases, however, the two solid sides of the meniscus may be able to coalesce and the solid bridge formed then will deform upon further pulling. Finally, when comparing SCN and metallic systems, it should be kept in mind that some differences exist, in particular the formation of last eutectic and oxides in most aluminium alloys.

Acknowledgements—The authors would like to thank Mr. J. Stramke, EPFL, for invaluable technical assistance in per-

forming the SCN experiments, Mrs. G. Berg, SINTEF, for assisting the SEM work, and Dr. Ch.-A. Gandin, EMN, for fruitful suggestions concerning the experiments. One of the authors (IF) has been funded by Hydro Aluminium, Elkem Aluminium, Hydro Raufoss Automotive Research Centre, and the Research Council of Norway through the project PROSMAT—Støperikompetanse.

REFERENCES

1. Pellini, W. S., *Foundry*, 1995, 125.
2. Guven, Y. F. and Hunt, J. D., *Cast Met.*, 1988, **1**, 104.
3. Campbell, J., *Castings*. Butterworth Heinemann, Oxford, 1991.
4. Clyne, T. W. and Davies, G. J., *Brit. Foundry.*, 1981, **74**, 65.
5. Feurer, U., *Gießerei-Forschung*, 1976, **28**, 75.
6. Rappaz, M., Drezet, J. -M. and Gremaud, M., *Met. Trans.*, 1999, **30A**, 449.
7. Farup, I. and Mo, A., *Met. Mater. Trans.*, 2000, **31A**, 1461.
8. Sigworth, G. K., *AFS Trans.*, 1999, **106**, 1053.
9. Nedreberg, M. L., Ph.D. thesis, University of Oslo, Dep. of Physics, February 1991.
10. Spittle, J. A. and Cushway, A. A., *Met. Technol.*, 1983, **10**, 6.
11. Drezet, J.-M., Ludwig, O. and Rappaz, M., *MECAMAT*, ed. Y. Berthaud, French Society of Metallurgy, LMT ENS, Cachan, France, 1999, p. 30.
12. Herfurth, Th. and Engler, S., in *Erstarrung metallischer Schmeltzen in Forschung und Gießereipraxis*, ed. A. Ludwig, DGM, Oberursel, Germany, 1999, p. 37.
13. Chopra, M. A., *Met. Trans.*, 1988, **19A**, 3087; *J. Cryst. Growth*, 1988, **92**, 543.
14. Farup, I. and Mo, A., *J. Therm. Stress.*, 2000, **23**, 71.
15. Prakash, O. and Jones, D. R. H., *Acta Metall.*, 1992, **40**, 3443.
16. Paradies, C. J., Smith, R. N. and Glicksman, M. E., *Met. Trans.*, 1997, **28A**, 875.
17. Glicksman, M. E., Schaefer, R. J. and Ayers, J. D., *Metall. Trans.*, 1976, **7A**, 1747.
18. Wulff, C. A. and Westrum, E. F. Jr., *J. Phys. Chem.*, 1963, **67**, 2376.
19. Fabietti, L. M., Seetharaman, V. and Trivedi, R., *Metall. Trans.*, 1990, **21A**, 1299.
20. Fabietti, L. M. and Sekhar, J. A., in *Nature and Porperties of Semi-Solid Materials*, eds J. A. Sekhar and J. Dantzig, 1991, p. 41.
21. Sémoroz, A., Henry, S. and Rappaz, M., *Met. Mater. Trans.*, 2000, **31A**, 487.